AD-A048 330 STANFORD UNIV CALIF CENTER FOR MATERIALS RESEARCH F/G 7/4
SOLID ELECTROLYTE BATTERY MATERIALS.(U)
NOV 77 R A HUGGINS N00014-76-C-0940
UNCLASSIFIED CMR-77-15 NL

END
DATE FILMED
2-78
DDC

(6)

OFFICE OF NAVAL RESEARCH

(15) Contract N00014-76-C-0940

Project NR 359-621

(9) FINAL REPORT,
1 Jul '76 - 31 Sep 77

(6) Solid Electrolyte Battery Materials.

(10) Robert A. Huggins
Principal Investigator
Department of Materials Science and Engineering

(11) November, 1977 (12) 15p.

Approved for Public Release; Distribution Unlimited

(14) CMR-77-15

Stanford University
Center for Materials Res.
Stanford, California

1473

400 827

1B

SECURITY CLASSIFICATION OF THIS PAGE (When Data Entered)

REPORT DOCUMENTATION PAGE

READ INSTRUCTIONS BEFORE COMPLETING FORM

1. REPORT NUMBER: Final Report	2. GOVT ACCESSION NO.
3. RECIPIENT'S CATALOG NUMBER	
4. TITLE (and Subtitle): Solid Electrolyte Battery Materials	5. TYPE OF REPORT & PERIOD COVERED: Final Report Through 9/31/77
	6. PERFORMING ORG. REPORT NUMBER: CMR - 77 - 15
7. AUTHOR(s): R. A. Huggins	8. CONTRACT OR GRANT NUMBER(s): N00014-76-C-0940
9. PERFORMING ORGANIZATION NAME AND ADDRESS: Stanford University, Stanford, CA 94305	10. PROGRAM ELEMENT, PROJECT, TASK AREA & WORK UNIT NUMBERS
11. CONTROLLING OFFICE NAME AND ADDRESS: Director, Chemistry Program, Office of Naval Research, 800 N. Quincy St., Arlington, VA 22217	12. REPORT DATE: November, 1977
	13. NUMBER OF PAGES
14. MONITORING AGENCY NAME & ADDRESS (if different from Controlling Office): ONR Resident Representative, Stanford University, Room 165 - Durand Aeronautics Bldg., Stanford, California 94305	15. SECURITY CLASS. (of this report): Unclassified
	15a. DECLASSIFICATION/DOWNGRADING SCHEDULE

16. DISTRIBUTION STATEMENT (of this Report)

Approved for Public Release; Distribution Unlimited

17. DISTRIBUTION STATEMENT (of the abstract entered in Block 20, if different from Report)

18. SUPPLEMENTARY NOTES

19. KEY WORDS (Continue on reverse side if necessary and identify by block number)

Solid electrolytes
lithium conductors
battery materials
ionic conductors
lithium nitride

20. ABSTRACT (Continue on reverse side if necessary and identify by block number)

This is the final report on this contract. Work involved the preparation of lithium nitride and a number of other potential ionic conductors and mixed ionic-electronic conductors. Most attention was given to lithium ionic conductors. Crystal structure information was obtained, and measurements made of ionic conductivity and other relevant properties.

DD FORM 1 JAN 73 1473 EDITION OF 1 NOV 65 IS OBSOLETE
S/N 0102-014-6601 |

SECURITY CLASSIFICATION OF THIS PAGE (When Data Entered)

INTRODUCTION

This is the final report on this contract, which started July 1, 1976 and ran through September, 1977. This program was a follow-on to some of the work undertaken under prior Contract N00014-75-C-1056, Project NR 056-555. Work involved the preparation of lithium nitride and a number of potential fast ionic conductors. Measurements of their crystallographic structure and ionic and electronic transport properties were also made.

Of special interest were the results on several new lithium ionic conductors, particularly polycrystalline Li_3N, which has been found to have unusually high lithium ion conductivity at ambient temperatures.

Another important result of this work has been the development of techniques for the analysis of the frequency dependence of ac impedance and admittance data on solid electrolytes and electrolyte-electrode systems to clearly separate and evaluate bulk transport and interface-related effects. It has also been shown that in some cases the separate influence of grain boundary and transcrystalline transport can be measured. This represents a significant step forward in the quantitative evaluation of mass and charge transport phenomena in materials with large values of ionic conductivity.

A total of 11 Technical Reports resulted from this work, and they have all also appeared in the technical literature. Three extensive review papers have also been (or are scheduled to be) published which relate, in part, to work supported under this contract. In addition, a paper on the most recent work on lithium nitride has been submitted for publication, but will not appear until the January issue of the Materials Research Bulletin.

A copy of this latter paper on lithium nitride, which shows that by

optimization of the microstructure one can achieve very high lithium ionic conductivity values in polycrystalline samples at ambient temperatures, comparable to those found in the "fast" direction in single crystals of this very anisotropic material, is included in this report.

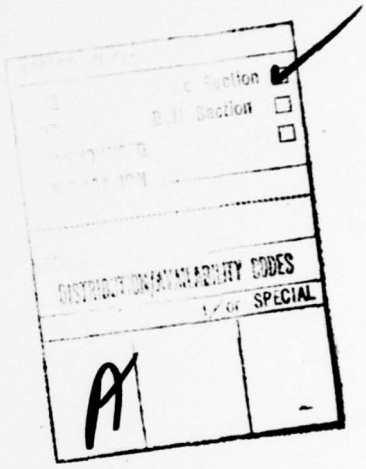

PUBLICATIONS RELATING TO THIS PROGRAM

I. D. Raistrick, C. Ho and R. A. Huggins, "Lithium Ion Conduction in Li_5AlO_4, Li_5GaO_4 and Li_6ZnO_4", Mat. Res. Bull. 11, 953 (1976). (Technical Report No. 1.)

B. A. Boukamp and R. A. Huggins, "Lithium Ion Conductivity in Lithium Nitride", Physics Letters A 58, 231 (1976). (Technical Report No. 2.)

W. Weppner and R. A. Huggins, "Ionic Conductivity of Alkali Metal Chloroaluminates", Physics Letters A 58, 245 (1976). (Technical Report No. 3.)

J. Schoonman, E. E. Hellstrom and R. A. Huggins, "Electrical Properties of $K_2FeCl_5 \cdot H_2O$ and K_2AlF_5", J. Solid State Chem. 18, 325 (1976). (Technical Report No. 4.)

I. D. Raistrick, Chun Ho and R. A. Huggins, "Ionic Conductivity of Some Lithium Silicates and Aluminosilicates", J. Electrochem. Soc. 123, 1469 (1976). (Technical Report No. 5.)

Y-W. Hu, I. D. Raistrick and R. A. Huggins, "Ionic Conductivity of Lithium Phosphate-Doped Lithium Orthosilicate", Mat. Res. Bull. 11, 1227 (1976). (Technical Report No. 6.)

R. A. Huggins, "Solid Electrolytes", in: Critical Materials Problems in Energy Production, Ed. Charles Stein, Academic Press (1976) p. 729.

W. Weppner and R. A. Huggins, "Ionic Conductivity of Solid and Liquid $LiAlCl_4$", J. Electrochem. Soc. 124, 35 (1977). (Technical Report No. 7.)

R. A. Huggins, "Ionically Conducting Solid State Membranes", in: Advances in Electrochemistry and Electrochemical Engineering, Vol. 10, Eds. Heinz Gerischer and Charles W. Tobias, John Wiley and Sons, Inc. (1977) p. 323.

I. D. Raistrick, C. Ho, Y-W. Hu and R. A. Huggins, "Ionic Conductivity and Electrode Effects on β-PbF_2", J. Electroanal. Chem. 77, 319 (1977). (Technical Report No. 8.)

R. A. Huggins, "Recent Results on Lithium Ion Conductors", Electrochimica Acta 22, 773 (1977). (Technical Report No. 9.)

I. D. Raistrick, N. Endow, S. Lewkowitz and R. A. Huggins, "Structural Aspects of Some Mixed Metal Ferrocyanides", J. Inorg. and Nucl. Chem. 39, 1779 (1977). (Technical Report No. 10.)

Y-W. Hu, I. D. Raistrick and R. A. Huggins, "Ionic Conductivity of Lithium Orthosilicate - Lithium Phosphate Solid Solutions", J. Electrochem. Soc. 124, 1240 (1977). (Technical Report No. 11.)

R. A. Huggins, "Crystal Structures and Fast Ionic Conductors", to be published in Solid Electrolytes, edited by W. van Gool and Hagenmüller, Pergamon Press.

B. A. Boukamp and R. A. Huggins, "Fast Ionic Conductivity in Lithium Nitride", to be published in Materials Research Bulletin (1978).

FAST IONIC CONDUCTIVITY IN LITHIUM NITRIDE

B. A. Boukamp and R. A. Huggins
Department of Materials Science and Engineering
Stanford University, Stanford, California 94305

ABSTRACT

Analysis of the frequency dependence of ac measurements with ionically-blocking electrodes, as well as transmission electron microscopic observations have enabled the transcrystalline and intercrystalline resistances of polycrystalline Li_3N to be separately evaluated. At 25°C the transcrystalline ionic conductivity is 6.6×10^{-4} (ohm cm)$^{-1}$ and the activation enthalpy is 24.1 kJ/mole. The intercrystalline conductivity has an activation enthalpy of 68.5 kJ/mole, and its magnitude varies with thermal history. By optimized thermal treatment, the microstructure can be controlled so the bulk conductivity becomes approximately equal to that for transport in the fast direction in this very anisotropic structure.

Introduction

In the search for solid electrolytes to be used in high energy or power density battery systems one of the criteria for selecting potential fast ionic conductors is the openness of the crystal structure. A number of solids with two-or three-dimensional "crystallographic tunnels" are known to be fast ionic conductors, such as the layer structure beta-alumina family (1,2), and materials with rigid skeleton structures such as $Na_3Zr_2PSi_2O_{12}$ (3). Similar behavior has also been found (4-11) in several materials with mobile cations in open tetrahedral polyanion arrays, and recently in a mixed conductor with one-dimensional tunnels (12).

From this point of view, Li_3N looks very promising, because of its unique open structure, which contains tightly bonded (13) Li_2N layers with the nitrogen in the center of hexagonal lithium arrays. These layers are connected by the remaining 1/3 of the lithium ions, which bridge between the nitrogen ions of adjacent layers. This arrangement was first proposed by Zintl and Brauer (14) and was recently reconfirmed by Rabinau and Schulz (15)

Although early work by Masdupuy (16,17) seemed to indicate a very low

ionic conductivity for Li_3N, later NMR studies of the ^7Li resonance by Bishop et al. (18) indicated very high Li ion mobility. In fact, the results of Masdupuy are subject to some doubt, as his conductivity measurements were evidently performed on loosely compacted powders.

This disparity led us to reinvestigate the ionic conductivity of this phase, and early results have been reported elsewhere (4,8,19). In this work we found that the thermal treatment of samples, as well as the methods used in their preparation, had significant effects upon both the magnitude and the temperature dependence of the apparent conductivity of polycrystalline samples. Subsequently, some measurements have been made on single-crystalline samples (20), which confirmed the high ionic conductivity, and demonstrated the expected large anisotropy in the ionic conductivity.

In this paper we report further experiments upon polycrystalline samples which were undertaken to study the previously observed annealing effects and to separately evaluate transcrystalline (bulk) and intercrystalline ionic transport. Because of the large anisotropy in the crystal structure, it was thought that comparison of polycrystalline and single crystal results might also prove interesting.

Synthesis of Li_3N

Several reports on the preparation of Li_3N from the elements have been published. According to Brauer (21) Li_3N can be made by reacting molten lithium in a ZrO_2 crucible, lined with LiF, with nitrogen gas diluted with argon at about 800°C. Kutolin et al. (22,23) described a method in which pure lithium ribbon was reacted with nitrogen at 6 atm pressure and 180°C for several hours.

We found that Li_3N can be made readily with nitrogen gas with a very low oxygen content at ambient pressure and moderate temperatures. A chunk of lithium was carefully cleaned by cutting off contaminated surfaces, and after weighing, placed in a molybdenum boat which was positioned in a stainless steel ampoule. The ampoule was then placed in a furnace and connected to the nitrogen supply. Oxygen was removed from the nitrogen by means of an electrochemical oxygen pump utilizing a tube of Ca-stabilized ZrO_2 closed at one end and provided with two Pt electrodes, one on the nitrogen side and one in contact with room air. The electrode area was kept at 750°C and polarized by 1.4 volts. In this way oxygen molecules that reached the Pt electrode on the nitrogen side were transported to the air through the ZrO_2 electrolyte. This system also reduces any water vapor present to oxygen and hydrogen, with the oxygen being removed from the gas stream. We do not know what influence the presence of a small amount of residual hydrogen might have had on the formation of Li_3N.

The temperature of the ampoule was slowly raised to about 180°C and kept there for several hours. If the temperature is raised too fast the reaction will proceed very rapidly, causing thermal runaway due to the strong exothermic reaction, thus melting the lithium.

The yield was weighed and the composition found to be $Li_{3.00 \pm .01}N$. The product was crushed and milled under nitrogen and then reheated in the stainless steel ampoule to ensure complete reaction with N_2. Reheating to 200°C resulted in a light brown powder, whereas reheating to 300°C or higher gives a bright red powder. The brown powder can be converted into the red powder by

later heating to 300°C, independent of the presence of nitrogen.

Polycrystalline Sample Preparation

Samples with densities up to 98% of theoretical were obtained by again remilling the heat treated Li_3N powder, followed by pressing and sintering. Pellets were pressed in an evacuable 3/8" diameter steel die at 2700 kg/cm^2 and sintered in purified nitrogen at temperatures between 650°C and 750°C. Ionically blocking electrodes were applied by sputtering a 0.3 μm layer of molybdenum on both sides of the pellets.

Conductivity Measurements

The complex impedance (or admittance) was measured in the frequency range .01 Hz to 20-100 kHz. The low frequency (.01 Hz - 20 Hz) measurements were carried out using a PDP 8E digital computer as a signal analyzer. The higher frequency range was measured using a model 1608 General Radio Impedance bridge or a specially designed arrangement (24) using a Princeton Applied Research Model 129 two phase lock-in amplifier, which extended the range to 100 kHz. To avoid amplitude-dependent nonlinearity, the ac voltage across the sample was kept below 50 mV peak to peak.

The pellets were placed between two spring-loaded molybdenum disc electrodes in a stainless steel conductivity cell. The ambient was purified nitrogen gas at approximately 1 atm pressure.

Analysis of the Frequency Dispersion of the Complex Impedance

Although the frequency dispersion of the complex impedance, or its inverse, the complex admittance, seemed to differ considerably for various Li_3N samples, it was possible, with careful analysis, to draw an equivalent circuit which described the form of all the data when its elements were properly adjusted.

In order to describe the frequency dispersion analysis, it is useful to start from the well-known Debye circuit, which is an idealized equivalent circuit that often is used as a first approximation in the analysis of the frequency dependence of the admittance/impedance of solid-blocking electrode combinations. This model (Fig. 1a) consists of an electrolyte-electrode interface capacitance, C_{int}, due to the ionically blocking electrodes, a bulk ionic resistance R_i, and the geometric capacitance C_{geom}, which is due to the simple parallel plate capacitance of the two electrodes, with the sample as a dielectric medium between them. If the solid is a reasonably good ionic conductor and the sample-electrode contact is good, the interface capacitance, C_{int}, is typically orders of magnitude larger than the geometrical capacitance. This then results in a clear separation of the frequency dispersion into a low frequency interface-related part (the vertical straight line, Fig. 1b) in which the behavior is dominated by a series combination of R_i and C_{int}, and a high frequency bulk-related part (the semicircle, Fig. 1b) in which the overall behavior is dominated by the parallel arrangement of R_i and C_{geom}. The opposite holds for the complex admittance plot (Fig. 1c), where the semicircle represents the low frequency part, and the tail the high frequency region.

The general form of the frequency dispersion of the complex impedance and admittance for the Li_3N samples at room temperature is shown in Figs. 2a and 2b, respectively. From this it is clear that the real behavior is more complex than that represented by the ideal Debye circuit. However, there is again a good separation between the low frequency part (the rising line in Fig. 2a)

and the high frequency part (the depressed and distorted semicircle). In contrast with the Debye circuit this distorted semicircle does not go through the origin in the complex impedance plane. Instead, it bends down to intersect the real axis. As discussed later, we found that this must be due to a second resistance in series with R_i in the equivalent circuit. We will discuss these two frequency ranges separately.

Low Frequency Region

That the low frequency region in the complex impedance represents the electrical response of the bulk in series with the electrode region was clearly shown by replacing the ionically blocking molybdenum electrodes with (reversible) lithium electrodes. It was then found that the low frequency dispersion region disappeared, as all low frequency points lay on top of each other on the real axis. This also indicated that the Li electrodes were kinetically reversible on the Li_3N in those experiments.

Computer analysis of the curvature of the low frequency portion of the dispersion curve using least squares fitting resulted in an equivalent circuit consisting of a bulk resistance, R_I, an interface capacitance, C_{int}, and a Warburg-like complex element, apparently related to diffusion processes near the electrolyte-electrode interface. The impedance of this complex element is of the form $Z_w = A\,\omega^{-\alpha} - j\,B\,\omega^{-\alpha}$, where α has values between 0 and 1, and it has been shown (25,26) that $B/A = \tan \alpha \frac{\pi}{2}$. The sign of the curvature indicated that the interface capacitance and the Warburg-like element are in series, rather than in parallel. The value of the interface capacitance was typically of the order of $1\text{-}2 \times 10^{-3}$ F/cm^2 at room temperature; it increased with increasing temperature and became immeasurably large at temperatures above 200°C. At the same time, the exponent α increased from about 0.5 to about 0.95, changing from a Warburg-dominated to a more capacitive behavior. This is in contrast with what has been found in other materials, such as single crystalline PbF_2, where the value of α remains constant over a wide range of temperature (26). The real and imaginary constants A and B of this Warburg element also changed with temperature, showing different activation energies (as the exponent α changes with temperature) of 27.0 and 19.3 kJ/mole, respectively. The physical processes underlying this behavior are not yet fully understood.

As reported earlier (19), the electronic conductivity is at least several orders of magnitude lower than that due to ionic transport in Li_3N.

High Frequency Region

The high frequency portion of the frequency dispersion varied greatly between different samples, and sometimes only part of the semicircle could be observed, due to the frequency limitations of the measuring equipment.

As mentioned earlier, one of the important differences from the simple ideal Debye model was the observation that the high frequency circular arc in the complex impedance plane did not extrapolate to the origin. This implies that there must be a second resistance in addition to R_i. In principle, this form of the frequency dispersion can be due to either a series or parallel arrangement of two resistances. However, from the temperature dependence of both apparent resistances, discussed later, it can be argued that only a series arrangement is applicable here. Thus the lower frequency resistance, which is designated as R_I in Fig. 2, represents the sum of the two resistances. The shape of the distortion of the circular arc indicates that the second resistance must also be in parallel with a frequency-dependent complex

impedance. The resulting equivalent circuit is shown in Fig. 3.

Interpretation of the Data

By analysis of the complex impedance plane data in terms of the equivalent circuit of Fig. 3, one readily obtains the values of the two resistances in series. The higher frequency intercept on the real axis R_{II} gives the value of one of them, and the lower frequency intercept R_I is the sum of the two. The resistance values were converted to conductivities, and evaluated as a function of temperature for samples which had undergone different thermal cycling and annealing schedules. Both resistance-causing phenomena were found to have an Arrhenius type of temperature dependence, following a relationship of the form $\sigma = (A/T) \exp(-\Delta H/RT)$.

It was found that the thermal history had very little effect upon either the magnitude or the temperature dependence of one of the resistances - the one corresponding to the higher frequency intercept in the complex plane plot.

On the other hand, the magnitude of the other resistance, which has a considerably greater activation enthalpy, varied significantly with thermal history. Cycling the temperature between ambient and 200°C caused it to increase, whereas more extensive annealing at relatively high temperatures (e.g., 750°C) caused it to decrease appreciably. The influence of high temperature annealing upon the measured conductivity values is shown in Fig. 4.

Observation of samples in the scanning electron microscope provided an explanation of this apparent contradiction. It was found that the low temperature cycling caused both transgranular and intergranular fractures to appear in the polycrystalline structure, undoubtedly related to the very anisotropic crystal structure, which is expected to also exhibit anisotropic thermal expansion.

On the other hand, high temperature annealing caused an appreciable amount of further sintering, thus increasing the area of intergranular contact. This change in the microstructure is illustrated in Fig. 5. It can be seen that, despite the anisotropic crystal structure, the Li_3N grains are reasonably equiaxed. These observations lead to the conclusion that the second (series) resistance has to do with the transport of lithium ions across the Li_3N grain boundaries. The conclusion that this resistance is related to intergranular phenomena is consistent with the fact that a complex capacitive impedance was also found to be associated with this resistance.

The transgranular lithium ion conductivity of these polycrystalline samples of Li_3N was found to have an activation enthalpy of 24.1 kJ/mole. At 25°C this component of the conductivity has a magnitude of about 6.6×10^{-4} $(\text{ohm cm})^{-1}$.

The series intergranular resistance, while changing in magnitude with thermal history, consistently was found to have an activation enthalpy of about 68.5 kJ/mole. The capacitive part of the complex grain boundary impedance varied with microstructural changes, as expected, from less than 1 nF for samples sintered at 650°C to 100-200 nF for samples sintered at 750°C.

Discussion

Lithium nitride is a very interesting material, with very large values of lithium ion conductivity. This work has shown that it is possible to clearly

separate the transcrystalline and intercrystalline components of ionic transport in bulk polycrystalline samples. The data extracted for the transcrystalline conductivity are quite close to those recently obtained for the ionic conductivity in the plane perpendicular to the c-axis in single crystals (20). Neither the overall conductivity nor the grain boundary phenomenon correspond to the single crystal data parallel to the c-axis.

The total bulk resistance of polycrystalline material is, of course, the sum of its transcrystalline and intercrystalline components. As a result, the lower of the two conductivities will dominate the overall behavior. Thus the temperature of the transition from transcrystalline to intercrystalline-dominated behavior of the polycrystalline material decreases as the structure becomes more fully sintered. It should also depend upon the grain size, although that parameter was not carefully explored in this work. While the data presented in Fig. 4 show that sintering at 750°C for 2 hours reduces the transition temperature to about 70°C, it should be possible to bring it below room temperature by giving careful attention to such microstructural control.

The readily visible, but relatively small, influence of intercrystalline or grain boundary resistance in dense well-sintered polycrystalline samples of Li_3N found here is similar to a number of previous observations on other fast ionic conductors. It is fortunate from a practical point of view, as it means that shapes may be fabricated of such materials by a number of different methods, and still have relatively high conductivity values.

In order to place these results in perspective, comparative data on the ionic conductivity of a number of lithium ion conductors are presented in Table I.

The practical applications of Li_3N may be limited, however, by its relatively low stability. Recent reports (27,28) have indicated that its free energy of formation is only 128.9 kJ/mole at 25°C, which limits the voltage that can be applied across it before decomposition to about 0.44 volts at 25°C, and somewhat less at higher temperatures.

Acknowledgement

This research was supported by the Office of Naval Research under Contract No. N00014-76-C-0940.

References

1. Y. F. Y. Yao and J. T. Kummer, J. Inorg. Nucl. Chem. 29, 2453 (1967).

2. M. S. Whittingham and R. A. Huggins, in "Solid State Chemistry", p. 139, ed. by R. S. Roth and S. J. Schneider, Nat. Bur. Standards Special Pub. 364, Washington (1972).

3. J. B. Goodenough, H. Y-P. Hong and J. A. Kafalas, Mat. Res. Bull. 11, 203 (1976).

4. B. A. Boukamp, I. D. Raistrick, C. Ho, Y-W. Hu and R. A. Huggins, in "Superionic Conductors", p. 417, ed. by G. D. Mahan and W. L. Roth, Plenum Press, New York (1976).

5. I. D. Raistrick, C. Ho and R. A. Huggins, Mat. Res. Bull. 11, 953 (1976).

6. W. Weppner and R. A. Huggins, Phys. Letters 58A, 245 (1976).

7. Y-W. Hu, I. D. Raistrick and R. A. Huggins, Mat. Res. Bull. 11, 1227 (1976).

8. R. A. Huggins, to be published in Electrochimica Acta.

9. R. D. Shannon, B. E. Taylor, A. D. English and T. Berzins, to be published in Electrochimica Acta.

10. W. Weppner and R. A. Huggins, J. Electrochem. Soc. 124, 35 (1977).

11. Y-W. Hu, I. D. Raistrick and R. A. Huggins, to be published in J. Electrochem. Soc.

12. B. E. Liebert and R. A. Huggins, to be published in Proceedings of Symposium on Electrode Materials and Processes for Energy Conversion and Storage, Electrochem. Soc. (1977).

13. H. Bilz, personal communication.

14. E. Zintl and G. Brauer, Z. Electrochem. 41, 102 (1935).

15. A. Rabenau and H. Schulz, J. Less Common Metals 50, 155 (1976).

16. F. Gallais and E. Masdupuy, Compt. Rendus 227, 635 (1948).

17. E. Masdupuy, Ann. Chimie, Paris, 13 Series 2, 1527 (1957).

18. S. G. Bishop, P. J. Ring and P. J. Bray, J. Chem. Phys. 45, 1525 (1966).

19. B. A. Boukamp and R. A. Huggins, Phys. Letters 58A, 231 (1976).

20. U. v. Alpen, A. Rabenau and G. H. Talat, to be published.

21. G. Brauer, "Handbuch der präp. anorg. Chemie, Vol. 2", p. 971, F. Enkle Verlag, Stuttgart (1962).

22. S. A. Kutolin and A. I. Vulikh, Prom. Khim. Reaktivov Osobo Chist. Veshchestv 13, 26 (1968).

23. S. A. Kutolin and A. I. Vulikh, Zh. Prikl. Khim. 41, 2529 (1968).

24. B. A. Boukamp and R. A. Huggins, to be published.

25. I. D. Raistrick, C. Ho and R. A. Huggins, J. Electrochem. Soc. 123, 1469 (1976).

26. I. D. Raistrick, C. Ho, Y-W. Hu and R. A. Huggins, J. Electroanal. Chem. 7, 319 (1977).

27. R. M. Yonco, E. Valeckis and V. A. Maroni, J. Nucl. Mat. 57, 317 (1975).

28. A. Bonomi, M. Hadate, and C. Centaz, J. Electrochem. Soc. 124, 982 (1977).

29. G. C. Farrington and W. L. Roth, in "Superionic Conductors", p. 418, ed. by G. D. Mahan and W. L. Roth, Plenum Press, New York (1976).

30. W. L. Roth and G. C. Farrington, Science 196, 1332 (1977).

31. C. Ho, I. D. Raistrick and R. A. Huggins, presented at American Ceramic Society Meeting, San Francisco (1976).

32. I. D. Raistrick, Y-W. Hu, C. Ho and R. A. Huggins, presented at Electrochemical Society Meeting, Philadelphia (1977).

33. J-M. Réau, A. Levasseur, G. Magniez, B. Calès, C. Fouassier and P. Hagenmuller, Mat. Res. Bull. 11, 1087 (1976).

34. J-M. Réau, G. Magniez, L. Rabardel, J-P. Chaminade and M. Pouchard, Mat. Res. Bull. 11, 867 (1976).

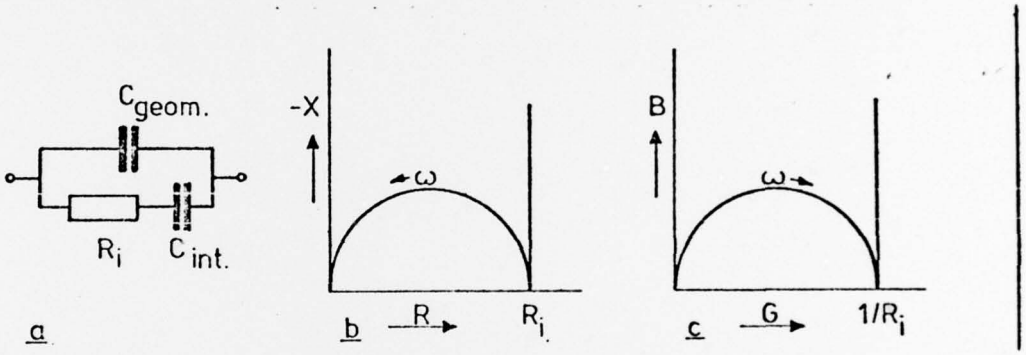

FIG. 1

a) Ideal Debye circuit, b) response of Debye circuit, plotted on complex impedance plane, c) response plotted on complex admittance plane.

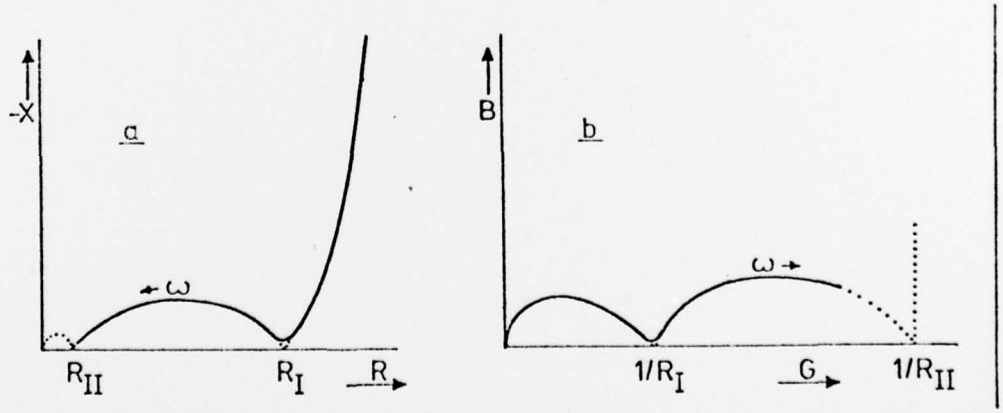

FIG. 2

General form of polycrystalline Li_3N data, plotted on: a) complex impedance plane, and b) complex admittance plane. $R_I = R_i + R_{GB}$, $R_{II} = R_i$.

TABLE I

Ionic Conductivity Data on Lithium Ionic Conductors

Material	σ at 25°C $(ohm\ cm)^{-1}$	σ at 450°C $(ohm\ cm)^{-1}$	References
Li_3N	6.6×10^{-4}	8.3×10^{-2}	This work
Li_3N (single crystal, ⊥ to c-axis)	1.2×10^{-3}	(1.5×10^{-1})	20
Li-β-alumina	1.3×10^{-4}	3.1×10^{-2}	2
Li, Na-β-alumina	5×10^{-3}	*	29,30
Li_5AlO_4	-	3.0×10^{-1}	4,5,8
Li_5AlO_4 + 20 m% Li_2SO_4	-	7.4×10^{-2}	31,32
Li_5AlO_4 + 67 m% Li_4SiO_4	-	5.8×10^{-2}	31,32
Li_4SiO_4 + 40 m% Li_3PO_4	1.7×10^{-6}	1.5×10^{-1}	4,7,8
Li_4SiO_4 + 60 m% Li_3PO_4	3.7×10^{-6}	1.7×10^{-1}	11
$Li_4B_7O_{12}Cl$	1.6×10^{-6}	8.0×10^{-2}	33
$Li_4B_7O_{12}Cl_{.68}Br_{.32}$	(4.6×10^{-7})	(1.5×10^{-3})	9
β-$Li\ Ta_3\ O_8$	(2.3×10^{-10})	1.5×10^{-2}	34

*Not stable

Values shown in parenthesis are extrapolated

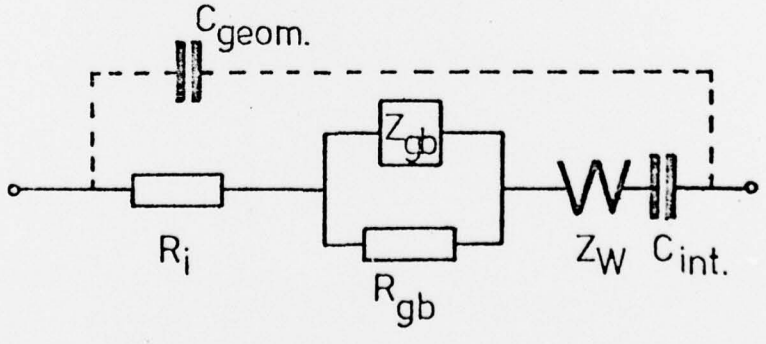

FIG. 3

Equivalent circuit that fits experimental data on polycrystalline Li_3N

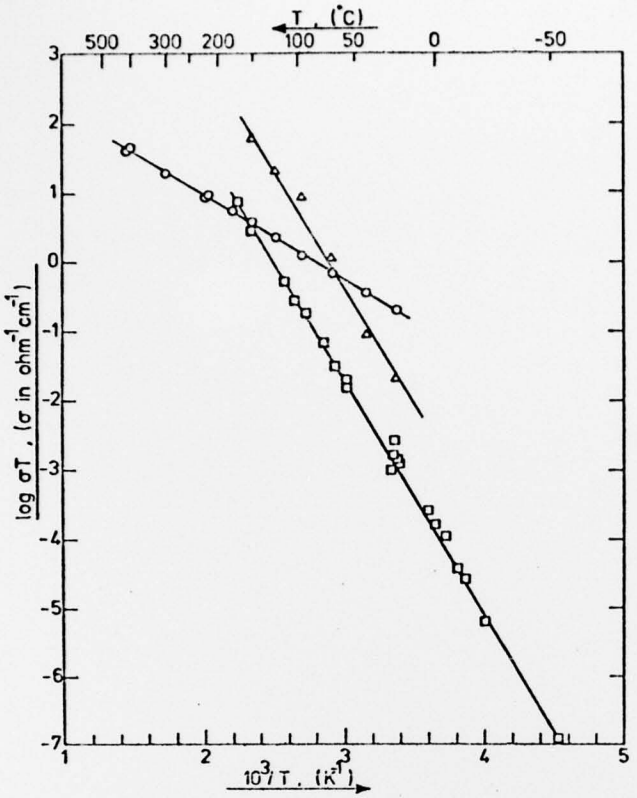

FIG. 4

Temperature dependence of transcrystalline (circles) and intercrystalline conductivity data. Lower values (squares) of intercrystalline conductivity after 1/2 hr anneal at 750°C, higher values (triangles) after 2 hr at 750°C

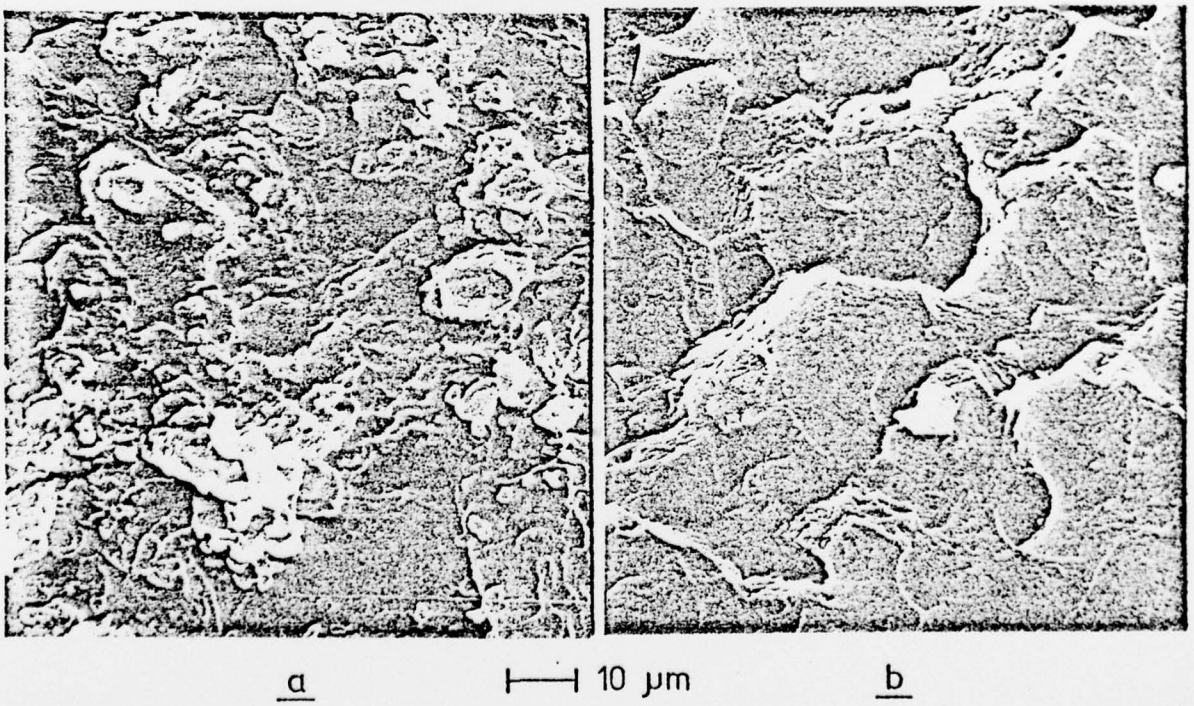

FIG. 5

Scanning electron microscope photographs showing microstructure after annealing a) 2 hr at 650°C, b) 2 hr at 750°C

TECHNICAL REPORT DISTRIBUTION LIST

	No. Copies
Office of Naval Research Arlington, Virginia 22217 Attn: Code 472	2
Office of Naval Research Arlington, Virginia 22217 Attn: Code 102IP	6
ONR Branch Office 536 S. Clark Street Chicago, Illinois 60605 Attn: Dr. George Sandoz	1
ONR Branch Office 715 Broadway New York, New York 10003 Attn: Scientific Dept.	1
ONR Branch Office 1030 East Green Street Pasadena, California 91106 Attn: Dr. R. J. Marcus	1
ONR Branch Office 495 Summer Street Boston, Massachusetts 02210 Attn: Dr. L. H. Peebles	1
Director, Naval Research Laboratory Washington, D.C. 20390 Attn: Library, Code 2029 (ONRL) Technical Info. Div. Code 6100, 6170	6 1 1
The Asst. Secretary of the Navy (R&D) Department of the Navy Room 4E736, Pentagon Washington, D.C. 20350	1
Commander, Naval Air Systems Command Department of the Navy Washington, D.C. 20360 Attn: Code 310C (H. Rosenwasser)	1

	No. Copies
Defense Documentation Center Building 5, Cameron Station Alexandria, Virginia 22314	12
U.S. Army Research Office P.O. Box 12211 Research Triangle Park, North Carolina 27709 Attn: CRD-AA-IP	
Commander Naval Undersea Research & Development Center San Diego, California 92132 Attn: Technical Library, Code 133	1
Naval Weapons Center China Lake, California 93555 Attn: Head, Chemistry Division	1
Naval Civil Engineering Laboratory Port Hueneme, California 93041 Attn: Mr. W. S. Haynes	1
Professor O. Heinz Department of Physics & Chemistry Naval Postgraduate School Monterey, California 93940	
Dr. A. L. Slafkosky Scientific Advisor Commandant of the Marine Corps (Code RD-1) Washington, D.C. 20380	1
ONR Branch Office One Hallidie Plaza - Suite 601 San Francisco, California 94102 Attn: Dr. P. A. Miller	1